

The Scattering and Absorption of π^+ Mesons by Aluminum

JAMES F. TRACY

Radiation Laboratory, Department of Physics, University of California, Berkeley, California

(Received March 16, 1953)

The interaction of π^+ mesons with aluminum has been studied in a magnet cloud chamber containing five $\frac{1}{8}$ -inch aluminum plates. Meson energies ranged from 25 to 100 Mev. 20 stops, 34 scatters $\geq 30^\circ$, and 57 stars were observed. A 1-prong star and a 70-Mev electron-positron pair in coincidence was interpreted as an inelastic charge-exchange scatter. All stops are reasonably accounted for by scatters and stars hidden by the geometry. The cross sections rise steeply with energy. The scattering (elastic plus inelastic) is very roughly isotropic except for a dip in the 60° to 90° interval. Corrected absolute cross sections for the 25-45-, 45-70-, and 70-100-Mev intervals, respectively, are $\sigma(\text{scat})$, 70 ± 23 , 312 ± 74 , and 216 ± 82 mb; $\sigma(\text{star})$, 176 ± 34 , 299 ± 62 , and 332 ± 100 mb; and $\sigma(\text{total})$, 246 ± 43 , 611 ± 95 , and 548 ± 129 mb. Detailed results and a description of experimental procedures are given.

INTRODUCTION

THE meson flux available and the estimated cross sections were such that it appeared profitable to undertake a cloud-chamber study of the interaction of pi-mesons with aluminum. A cloud-chamber study has the advantage of providing more detailed information concerning individual events than do other techniques. Aluminum met the need for a fairly light (low Z) nucleus to minimize Coulomb scattering and is a solid easily handled in a cloud chamber.

Many workers have been studying meson interactions. There is now a considerable amount of data on both interactions with nucleons and with complex nuclei. Much more data are still needed, of course, to

fill in and extend the broad outlines of current knowledge. For an excellent review article and an extensive bibliography of the experimental work in meson physics through 1950, see Marshak.¹ References to some of the more recent work will be made later. A more detailed account of the present investigation is available elsewhere.²

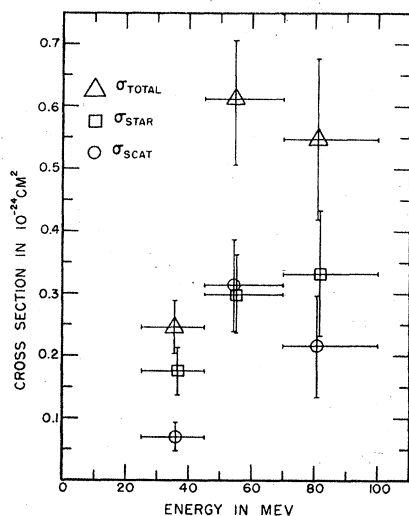


FIG. 1. Absolute cross sections for the interaction of positive pions with aluminum. The data are based upon 111 events, which included scatters $\geq 30^\circ$ stars and stops. The stops have been apportioned between the scatters and stars in accordance with calculated geometrical corrections. The scattering cross sections have been extended to include the angles from 0° to 30° by using the average differential cross section between 30° and 180° to obtain a total scattering cross section over 4π steradians. No distinction between elastic and inelastic scattering events has been attempted. Standard deviations, based upon statistics only, and energy groupings are indicated for the abscissas and ordinates, respectively ($\sigma_{\text{total}} = \sigma_{\text{star}} + \sigma_{\text{scat}}$).

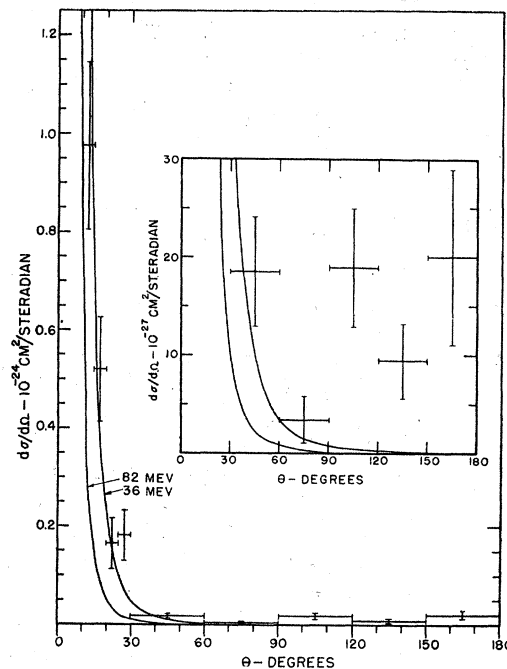


FIG. 2. Differential cross sections for scattering of positive pions by aluminum. The plotted points are experimental values based upon 114 scatters between 10° and 180° (34 , between 30° and 180°) of pions having energies between 25 and 100 Mev (mean energy = 49 Mev). Standard deviations, based upon statistics, and angular groupings are indicated. The solid curves represent theoretical single Coulomb scattering at two different energies for comparison purposes. The inset reproduces a portion of the same data to an enlarged ordinate scale.

¹ R. E. Marshak in *Annual Review of Nuclear Science* (Annual Reviews, Inc., Stanford, 1952), Vol. I.

² J. F. Tracy, University of California Radiation Laboratory Report UCRL-2013, 1952 (unpublished).

TABLE I. Data on the interaction of 25–100-Mev positive pions with aluminum.^a

Energy interval (Mev)	Observed number of events				Corrected number of events			Absolute cross sections (corrected for geometry and mu-contamination) (millibarns)		
	Stops n_0	Scatters $\geq 30^\circ$ n_S	1-prong stars n_1	2-prong stars n_2	Scatters $\geq 30^\circ$ N_S	1-prong stars N_1	2-prong stars N_2	Scattering σ_{scat}	Star production σ_{star}	Total σ_{total}
25–45	9	9	18	5	10.6	14.2	14.5	70±23	176±37	246±43
45–70	8	18	10	13	25.1	8.2	17.3	312±74	299±62	611±95
70–100	3	7	6	5	7.9	6.8	6.2	216±82	332±100	548±129
(Total)										
25–100	20	34	34	23	43.6	29.2	38.0	162±28	234±31	396±41

^a The definition of symbols is given in Appendix II. Elastic and inelastic scatters have not been separated. The absolute cross sections have been corrected for events hidden by geometry and for the error in the pion count introduced by the muon contamination. The absolute scattering cross sections have been computed by extending the average differential cross section for scatters $\geq 30^\circ$ over the total solid angle of 4π steradians. The indicated uncertainties are standard deviations based upon numbers of events only. Most of these cross sections are presented graphically in Fig. 1.

TABLE II. Data on the scattering of 25–100-Mev positive pions by aluminum.^a Scattering angle $-\theta$ (angular interval in degrees).

Energy interval (Mev)	10–15	15–20	20–25	25–30	30–60	60–90	90–120	120–150	150–180	30–180
Number of scatters actually observed										
25–45	24	16	8	7	3	1	2	1	2	9
45–70	8	6	2	3	5	0	7	4	2	18
70–100	1	2	0	3	3	1	1	1	1	7
(Total)										
25–100	33	24	10	13	11	2	10	6	5	34
Number of scatters after correction for those hidden by geometry										
25–45	24.0	16.0	8.0	7.0	3.1	1.5	3.0	1.0	2.0	10.6
45–70	8.0	6.0	2.0	3.0	5.9	0.0	12.9	4.3	2.0	25.1
70–100	1.0	2.0	0.0	3.0	3.1	1.6	1.2	1.0	1.0	7.9
(Total)										
25–100	33.0	24.0	10.0	13.0	12.1	3.1	17.1	6.3	5.0	43.6
Corrected differential scattering cross section $-d\sigma/d\Omega$ (millibarns/steradian)										
(Total)	976	520	165	182	18.5	3.4	18.9	9.4	20.0	12.9
25–100	±170	±106	±52	±50	±5.6	±2.4	±6.0	±3.8	±8.9	±2.2

^a Elastic and inelastic scatters were not distinguishable and have not been separated. The differential scattering cross sections have been corrected for scatters hidden by the geometry and for the error in the pion count introduced by the muon contamination. The indicated uncertainties are standard deviations based upon numbers of events only. These cross sections are presented graphically in Fig. 2. It will be noted that the right-hand column includes all scatters $\geq 30^\circ$. The differential cross section in the right-hand column is, thus, the average for all angles $\geq 30^\circ$. The total counts in the 10°–15° and 15°–20° intervals should probably be reduced by two each, as a correction for π - μ decays.

RESULTS

The results are presented graphically in Figs. 1 and 2 and numerically, in more detail, in Tables I, II, and III. Additional information is set forth below. The data presented in this paper refer to the laboratory system. This is essentially the same, however, as the center-of-mass system because the mass of the aluminum nucleus is so much greater than the meson mass.

It is apparent that the absolute scattering, star, and total cross sections (Fig. 1 and Table I) have a rapid rise with energy and that the total cross section equals the nuclear area [$=(\pi A)^{1/2} \approx 550$ millibarns, $r \approx 1.4 \times 10^{-13}$ cm] in the 60-Mev region and drops to half this value near 30 Mev. It is not clear whether it continues to rise, levels off, or eventually drops down again beyond 60 Mev. The star production cross section is about half again as large as the (elastic plus inelastic) scattering cross section.

Within the statistics, it appears possible to characterize the nuclear scattering as isotropic, although

there is definite indication of a minimum between 60° and 90°. This minimum may be attributable to diffrac-

TABLE III. Data on the total amount of aluminum traversed by the meson beam.^a

Energy interval (Mev)	Mean energy (Mev)	Total path of accepted tracks (g/cm ² Al)	Correction for muon contamination (g/cm ² Al)	Corrected path (g/cm ² Al)	Cross section per event (millibarns)
25–45	36.1	7.800	498(±33%)	7.300(±2%)	6.14
45–70	54.7	5.180	1.350(±33%)	3.830(±12%)	11.7
70–100	81.5	2.330	570(±33%)	1.760(±11%)	25.5
(Total)					
25–100	49.3	15.310	2.420(±33%)	12.890(±6%)	3.48

^a By "mean energy" (second column) is meant the average energy with respect to g/cm² of aluminum traversed. The uncertainty in total (uncorrected) path is less than one percent. The 33 percent mu-contamination uncertainty is an estimated maximum. The "cross section per event" (right-hand column) was computed by assuming one event over the corrected path in each energy interval; the uncertainties are those of the corrected paths. These data, when multiplied by the appropriate numbers of events, give the respective cross sections in Tables I and II. (The total number of acceptable tracks upon which the above data are based was 3976, corresponding to 15 359 plate traversals.)

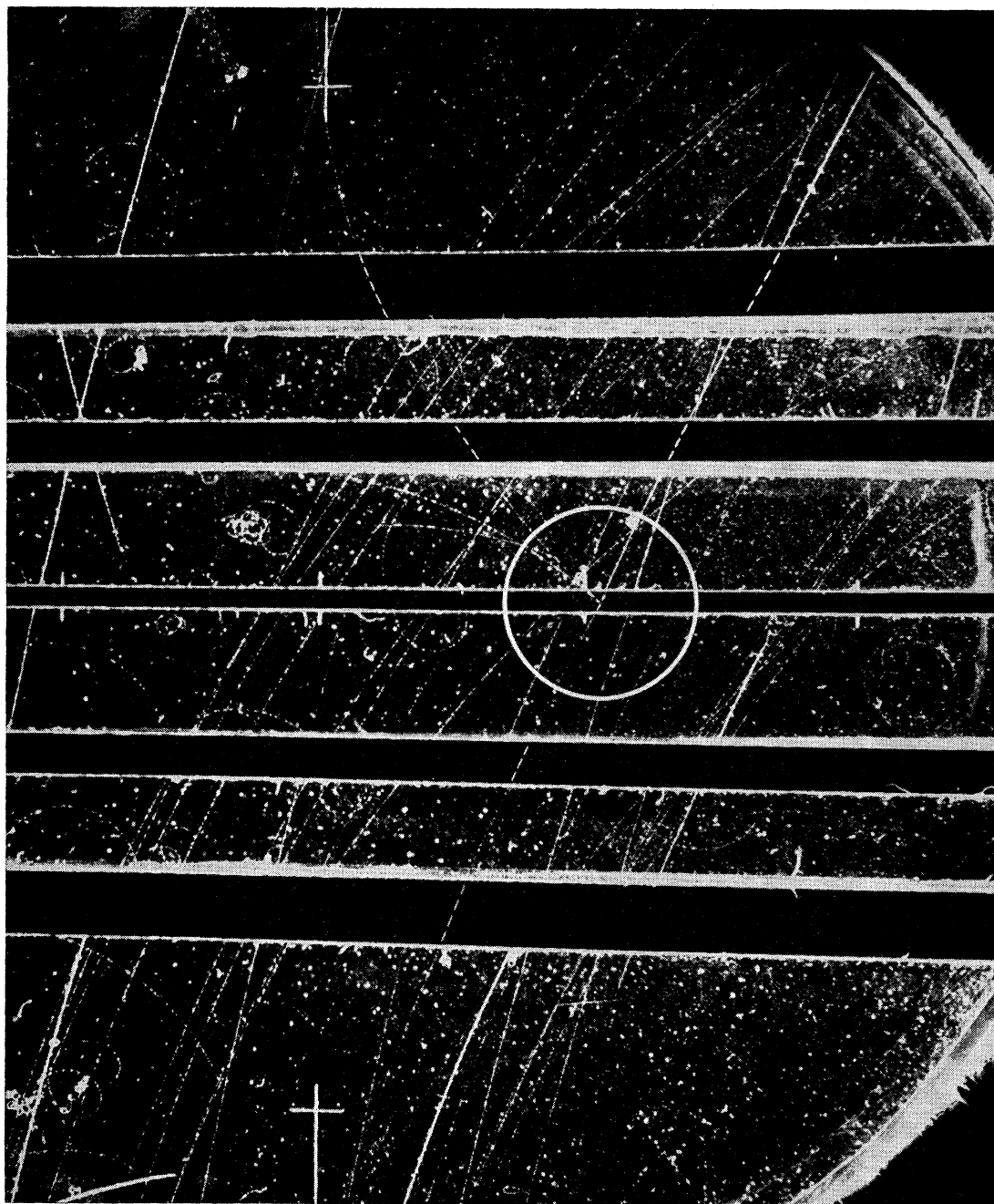


FIG. 3. A charge-exchange scatter. An 88-Mev pion enters the third plate and, presumably, suffers a charge-exchange scatter. A 51-Mev proton is ejected at 6° to the forward direction; the neutral pion decays and causes a 70-Mev electron-positron pair to leave the plate at 75° to the forward direction. (The electron takes 28 Mev and the positron, 42 Mev.)

tion effects in accord with the optical model of the nucleus proposed by Fernbach, Serber, and Taylor.³⁻⁵ The differential scattering cross section, averaged over all energies and all angles $\geq 30^\circ$, is 12.9 ± 2.2 millibarns (Table II). The small angle scattering follows the

³ Fernbach, Serber, and Taylor, Phys. Rev. 75, 1352 (1950).

⁴ H. A. Bethe and R. R. Wilson, Phys. Rev. 83, 690 (1951).

⁵ Byfield, Kessler, and Lederman, Phys. Rev. 86, 17 (1952).

theoretical single Coulomb scattering predictions reasonably well. The data are too coarse to draw conclusions about the interference between Coulomb and nuclear scattering.

In Table I, stars are listed as either 1 prong or 2 prong. Among the stars listed as 2 prong included is one that actually had three prongs and another that had four prongs. It is presumed that many of the stars

emitted more than two ionizing fragments but that these additional fragments were too slow to escape the aluminum plates. Of the 83 star prongs that were observed, 49 were "fast" and 34 were "slow." The great majority of prongs appeared to be protons; for purposes of estimating prong energies, all were assumed to be protons. Fast protons were those estimated to have energies >30 Mev and slow prongs were those estimated to have energies <30 Mev. The angular distribution of the fast prongs was isotropic; their forward-to-backward ratio being 24:25. The slow prongs, on the other hand, were predominantly forward; their forward-to-backward ratio being 25:9.

It is of interest to note the number of 2-prong stars whose prongs were in approximately opposite directions. Altogether, there were five stars in which the prongs were opposite to within 30° . In three cases, where both prongs were fast, the included angle between the two prongs differed from 180° by 16° , 28° , and 30° , respectively. In two other stars, having one fast prong and one slow prong, the included angle differed from 180° by 16° and 29° , respectively. This two-proton phenomenon has been reported before,^{5,6} and it has been

pointed out that this is evidence favoring a model proposed by Brueckner, Serber, and Watson.⁷ These authors have suggested that the positive pion is absorbed by a neutron in the nucleus, and the recoil is taken up by an adjacent nucleon. The neutron-turned proton and the recoiling nucleon are ejected in opposite directions from their position in the nuclear structure with 70 Mev of kinetic energy each. If the recoiling nucleon is a proton then two oppositely-moving protons may be seen to emerge.

Of the many events photographed in the chamber, only one was strikingly unusual. It is shown in Fig. 3. An 88-Mev pion entered the third plate and a proton of approximately 51 Mev was ejected nearly straight forward ($\theta=6^\circ$). In coincidence with this "1-prong star" is a 70-Mev electron-positron pair. This event is interpreted as an inelastic charge-exchange scattering event ($\pi^+ + n \rightarrow p + \pi^0$). The decay of the resultant neutral pion is presumed to have given rise to the electron pair. This event might also be interpreted as a radiative capture process ($\pi^+ + n \rightarrow p + \gamma$), wherein the photon is converted into an electron-positron pair in the aluminum. As Rankin and Bradner⁸ have pointed

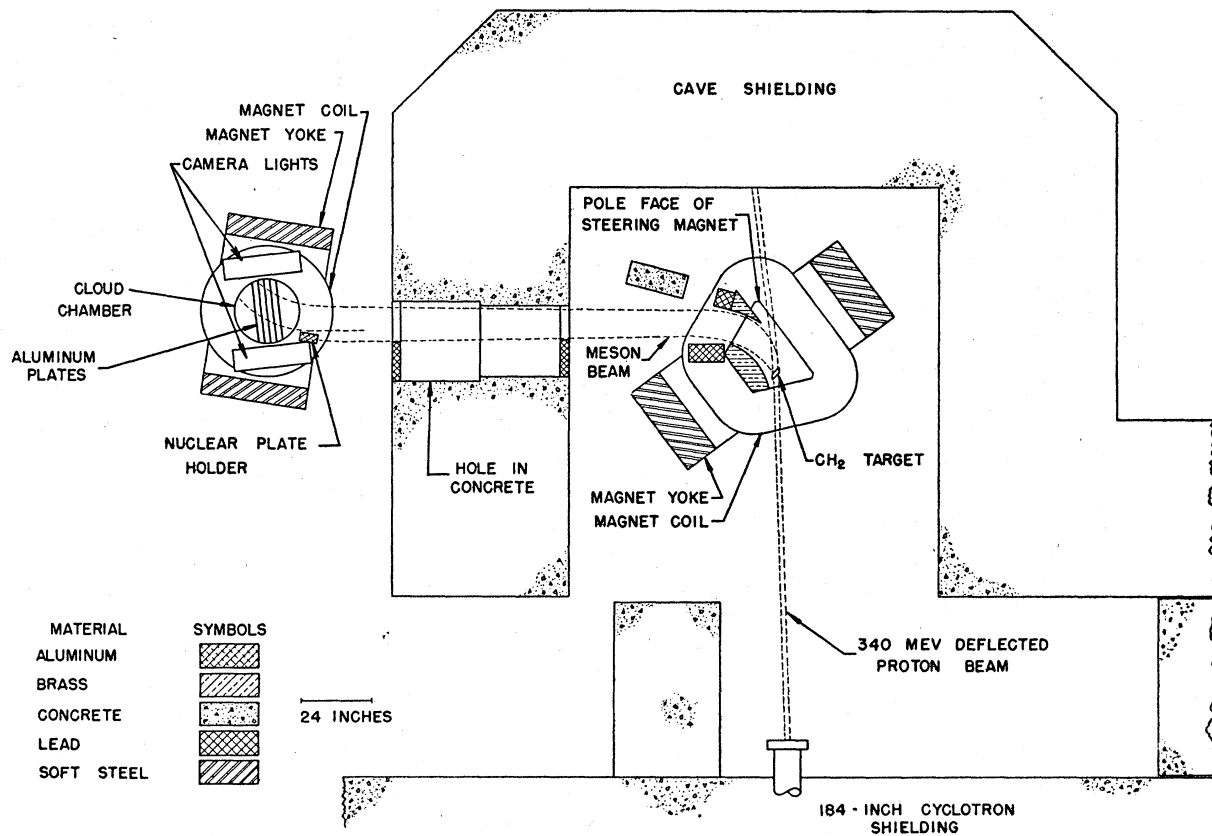


FIG. 4. Experimental arrangement.

⁵ G. Bernardini and F. Levy, Phys. Rev. 84, 610 (1951).

⁷ Brueckner, Serber, and Watson, Phys. Rev. 84, 258 (1951).

⁸ B. Rankin and H. Bradner, Phys. Rev. 87, 553 (1952).

out, this latter eventuality is very unlikely. The inverse photomeson production cross section is extremely small,⁹ and one can infer from detailed balancing arguments that the inverse radiative capture process is likewise extremely unlikely.

The coincidence of the 1-prong star and the pair could hardly have been accidental. One can estimate the probability of an accidental coincidence from the fact that perhaps 30 high-energy pairs occurred in the 600-odd pictures scanned. If one assumes conservatively that a pair and a star have to intersect within the same 0.2-inch square section of aluminum plate before appearing to be in "coincidence," then the accidental rate per star is 10^{-5} . This probability is reduced still more when one considers that all other pairs seen in the chamber pointed back toward the CH_2 target (Fig. 4). The pair in Fig. 3 is almost at 90° to the target direction and could not have been created by a gamma-ray from that source.

One can only conclude that the pair was the result of a π^0 decay associated with the 1-prong star. (Since the π^0 mean life is less than 5×10^{-14} sec,¹⁰ it could not have traveled more than 10^{-3} cm before decaying.) The π^0 's usual mode of decay is into two photons, each of 70 Mev in the center-of-mass system. A radiation length in aluminum is 9.7 cm, and it may be readily supposed that the one electron-positron pair observed is the only conversion that occurred among possibly 100 photons resulting from half that number of charge-exchange scatters. It is thus entirely possible that a number of the other 1-prong stars observed were also associated with inelastic charge-exchange scatters.

The pair might also have arisen directly from the neutral pion decay.¹¹ Steinberger¹² has very recently found that two percent of π^0 decays result directly in an electron pair and a single gamma, in competition with the two-gamma process.

DISCUSSION

It is useful to consider the nuclear absorption of pions which come to rest in matter because of the insight given into the nuclear interaction of mesons in flight. A stopped negative pion is essentially always captured by a nucleus. Once inside the nucleus the meson may be considered to be captured by a proton which is part of, say, a deuteron or an alpha-particle subgroup.^{13,14} The proton is transformed into a neutron ($\pi^- + p \rightarrow n + \text{K.E.}$) that receives, as kinetic energy, half of the 140-Mev meson rest mass. Momentum conservation requires that another particle in the subgroup, either a neutron or a proton, receive the other half of the 140 Mev. Thus in the primary absorption event

two fast nucleons, moving in opposite directions and each with about 70-Mev energy, are created. These may escape directly, leaving the residual nucleus with only a small excitation, or both primary nucleons may suffer energy degradation by collisions with other nucleons on the way out causing one or two additional fast nucleons to be ejected, and/or leaving the residual nucleus in a highly-excited state. This residual excitation can be dissipated by the subsequent "boiling off" of slower fragments. One of the primary fast nucleons is always a neutron and often the other is also. In this latter event both neutrons may escape without collisions, or may make only collisions yielding additional neutrons. When no ionizing particles are emitted, such an event will appear as a meson disappearance or "stop."

The consequence of the absorption by a nucleus of a 50-Mev "fast" meson should not be too different from those of the absorption of a "slow" meson after coming to rest. The meson rest mass will still be the major contributor to the energy released. Here there is, however, the possibility of the absorption of positive as well as negative pions, because the repulsive Coulomb potential barrier is now low relative to the pion kinetic energy. From charge-symmetry considerations, one expects positive pion events to "mirror" negative pion events, i.e., neutrons to replace protons, and vice versa. In the case of fast mesons, of course, one expects scattering events as well as absorption events.

Recent work of other investigators includes successful attacks using electronic techniques on meson interactions with "free" nucleons,¹⁵⁻²² in addition to studies using various techniques on interactions with complex nuclei.^{5,6,8,20-25} One group has used the diffusion cloud chamber for meson-proton and meson-alpha-particle experiments.^{26,27}

Most experimenters have used pions in the energy range between 50 and 100 Mev. Work with negative pions predominates. The general features of pion interactions with complex nuclei are shared by both positive and negative varieties. The total cross sections (in the above-mentioned energy interval) are approxi-

¹⁵ Durbin, Loar, and Steinberger, *Phys. Rev.* **84**, 581 (1951).

¹⁶ Isaacs, Sachs, and Steinberger, *Phys. Rev.* **85**, 803 (1952).

¹⁷ Anderson, Fermi, Long, Martin, and Nagle, *Phys. Rev.* **85**, 934 (1952).

¹⁸ Anderson, Fermi, Long, and Nagle, *Phys. Rev.* **85**, 936 (1952).

¹⁹ Anderson, Fermi, Nagle, and Yodh, *Phys. Rev.* **86**, 413 (1952); **86**, 793 (1952).

²⁰ Chedester, Isaacs, Sachs, and Steinberger, *Phys. Rev.* **82**, 958 (1951).

²¹ Martin, Anderson, and Yodh, *Phys. Rev.* **85**, 486 (1952).

²² R. L. Martin, *Phys. Rev.* **87**, 1052 (1952).

²³ Bernardini, Booth, and Lederman, *Phys. Rev.* **83**, 1075 (1951); **83**, 1277 (1951).

²⁴ H. Bradner and B. Rankin, *Phys. Rev.* **87**, 547 (1952).

²⁵ Camac, Corson, Littauer, Shapiro, Silverman, Wilson, and Woodward, *Phys. Rev.* **82**, 745 (1951).

²⁶ Shutt, Fowler, Miller, Thorndike, and Fowler, *Phys. Rev.* **84**, 1247 (1951).

²⁷ Thorndike, Fowler, Fowler, and Shutt, *Phys. Rev.* **85**, 929 (1952).

⁹ J. Steinberger and A. S. Bishop, *Phys. Rev.* **86**, 171 (1952).

¹⁰ Carlson, Hooper, and King, *Phil. Mag.* **41**, 701 (1950).

¹¹ Lord, Fainberg, Haskin, and Schein, *Phys. Rev.* **87**, 538 (1952).

¹² J. Steinberger to J. V. Lepore, private communication.

¹³ D. H. Perkins, *Phil. Mag.* **40**, 601 (1949).

¹⁴ S. Tamor, *Phys. Rev.* **77**, 412 (1950).

mately equal to the nuclear areas (geometrical cross sections); inelastic events (i.e., absorptions and inelastic scatters) occur somewhat more frequently than elastic (scattering) events; and there is a high probability for large angle, single scatters. There is at least one marked difference between the two signs, however. A large fraction of negative pion and few, if any, positive pion absorption events are disappearances. This difference may be understood by noting that a positive pion always produces within the nucleus at least one fast proton, while a negative pion similarly always produces at least one neutron. When the second fast nucleon, is likewise a neutron, the negative pion may suffer a disappearance.

More recently, especially with observations on hydrogen and deuterium, it has been found that the total cross sections increase rapidly with energy up to energies of 100 or more Mev.^{6,15,17,18,22} Somewhere beyond 100 Mev the cross sections begin to level off. At very high energies, at 920 Mev, as obtained in cosmic rays, the total cross sections on carbon and lead have dropped down to about 75 percent of the nuclear area.²⁸

The results obtained in the present experiment (Figs. 1 and 2, and Tables I and II) are in general agreement with the statements made above. A direct comparison with the published data on total cross sections for aluminum can be made. Camac *et al.*,²⁵ apparently using equal numbers of positive and negative pions of about 45 Mev, obtained 480 ± 140 mb; Chedester *et al.*,²⁰ using 85-Mev negative pions, obtained 623 ± 25 mb; and Martin *et al.*,²¹ using 109-Mev and 133-Mev negative pions, obtained 590 ± 60 mb and 580 ± 50 mb, respectively. The author's results are in agreement with these data. It will be noted that the results of Martin *et al.* indicate a leveling off somewhere beyond 100 Mev.

Camac *et al.* have also separated star events from scattering events. They did not distinguish between scatters and single-prong stars (they lumped these together) because the two kinds of events, in the absence of a magnetic field, had similar appearances in their cloud chamber. With this restriction, they observed six stars and nine scatters $> 20^\circ$, which is in rough agreement with the author's corrected data; i.e., 38 2-prong stars and 73 1-prong stars plus scatters $\geq 30^\circ$.

Byfield *et al.*⁵ have made a magnet cloud-chamber study of both negative and positive 62-Mev pions on carbon. They have distinguished elastic from inelastic scatters and, for positive pions, have obtained $\sigma(\text{star}) = 153 \pm 22$ mb, $\sigma(\text{elastic scattering}) = 89 \pm 10$ mb, and $\sigma(\text{inelastic scattering}) = 15 \pm 8$ mb. If their elastic and inelastic scattering cross sections are combined, one finds the ratio of star events to scattering events to be 3:2. This is precisely the ratio the author has obtained

for aluminum. A further interesting comparison can be made: Byfield *et al.* list the proton star prongs > 40 Mev. The ratio of number of fast prongs to number of stars is 161:153 (=1.05). The like quantity for the author's experiment is 49:67 (=0.73). This difference between carbon and aluminum is not surprising; fast protons are more likely to suffer collisions and to be more degraded in energy when leaving the larger nucleus-aluminum.

In the present work, all of the 20 stops observed (i.e., disappearances—see Table I) were assumed not to be true disappearances but rather stars and scatters that were hidden by the geometry. This assumption seems reasonable as all of the observed stops can be accounted for by the geometrical corrections applied to the observed stars and scatters. The validity of the assumption is further substantiated by the work of others in studies of fast positive pions in emulsions. Bernardini and Levy⁶ observed no disappearances in the course of finding 41 scatters $> 40^\circ$ and 118 stars. Similarly, Rankin and Bradner⁸ discovered no disappearances while finding five scatters $> 30^\circ$ and 11 stars.

EXPERIMENTAL PROCEDURE

Positive ions of about 50-Mev energy were produced by bombarding a polyethylene (CH_2) target with the 340-Mev pulsed proton beam of the 184-inch Berkeley cyclotron and were then channeled into an array of five parallel aluminum plates inside a Wilson cloud chamber placed in a 5200-gauss magnetic field. Meson-induced events occurring in the chamber were recorded by a stereoscopic camera. These stereoscopic photographs were then reprojected upon a movable screen in a manner permitting the original three-dimensional configuration of events to be observed and measured. By a sampling procedure, the energy spectrum and total path lengths for mesons traversing the aluminum plates were determined. Finally, after counting the events, applying certain geometrical weighting factors, and making allowances for contaminating particles in the pion beam, the desired scattering and absorption cross sections were obtained. The details of this procedure are outlined in what follows.

Production and Recording of Events

The experimental arrangement is indicated in Fig. 4. The pions were produced in an arrangement used by Richman, Skinner, Merritt, and Youtz.²⁹ The steering magnet turned the mesons through 90° into an 8×24 -inch tunnel in the concrete shielding from whence they entered the cloud chamber outside. The meson trajectories were surveyed by means of a flexible stranded copper wire subject to a measured tension and carrying a predetermined electric current to simulate a particular meson momentum. The meson beam was defined by careful collimation to minimize the number of protons

²⁸ R. L. Cool and O. Piccioni, Phys. Rev. **87**, 531 (1952).

²⁹ Richman, Skinner, Merritt, and Youtz, Phys. Rev. **80**, 900 (1950.)

and decay muons entering the chamber. The spectrum of meson energies is indicated in Fig. 5.

The Wilson cloud chamber used was developed by Powell.³⁰ It is 22 inches in diameter, has a sensitive region $3\frac{1}{2}$ inches deep, was filled with about one atmosphere of argon gas, and was operated in a 5200-gauss magnetic field. 5200 gauss was a compromise. A higher field was desirable to increase the curvature of the mesons and thus make possible more accurate measurements of their momentum; a lower field was needed to reduce the curvature in order that mesons might more readily enter the chamber and also has the advantage of permitting a more accurate measurement of scattering angle. The plates used were of 2S commercially pure aluminum, which has a minimum purity of 99 percent. The plates were $\frac{1}{8}$ inch (0.858 g/cm²) thick and spaced at two-inch intervals.

Measurement and Reduction of Data

All counting and measuring of events was done with a special stereoscopic projector developed for the general use of the Radiation Laboratory cloud-chamber group, under Powell.³¹ The geometrical criteria by which meson tracks and events were accepted are discussed here. The section on "Meson Beam Contamination" states the means by which mesons were distinguished from heavier particles, and the manner in which positron and mu-contaminations were handled. Acceptable tracks were required to lie well within the illuminated region, to have sufficient track length before the first plate to permit good curvature measurements, and to

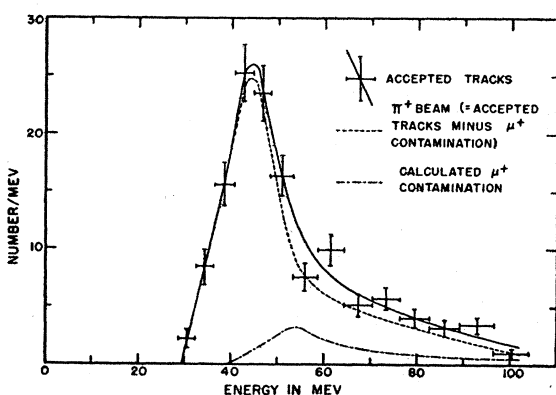


FIG. 5. Energy spectra for the meson beam at the cloud chamber. These data are based upon a sample of 628 accepted tracks measured before the first plate. Accepted tracks satisfied certain criteria regarding ionization, position, and direction intended to identify them as positive pions, but which did not exclude positrons and positive muons of acceptable $B\rho$. Positron contamination was negligible. The energies plotted for the μ^+ contamination are the energies of pions having the calculated muon $B\rho$'s. Standard deviations and energy groupings are indicated for the accepted tracks.

³⁰ W. M. Powell, Rev. Sci. Instr. 20, 403 (1949).

³¹ Brueckner, Hartsough, Hayward, and Powell, Phys. Rev. 75, 555 (1949).

satisfy certain conditions regarding the horizontal and vertical angles with which they entered the first aluminum plate. Figure 6 serves to illustrate how the first plate was divided into four intervals, I to IV, for the purpose of grouping the incoming tracks. Tracks passing to the left of I or the right of IV were considered too short (they were less than 7 cm long) for good curvature measurements. The vertical white lines near the left end of each plate indicate the points beyond which a track traversal was not counted; meson scatters or star fragments originating to the left of these lines were considered likely to be overlooked.

The acceptable values for the vertical (dip) angle α were taken to be those within $\pm 3^\circ$ of the horizontal. All but two or three percent of the otherwise acceptable tracks lay within this range; those outside were considered more likely to be muons from the decay of pions in flight than pions, themselves. The acceptable range for values of the horizontal (beam) angle β at the first plate was determined in the following way: The tracks were separated into groups I to IV, according to their point of entry into the first plate. Tracks within each group were divided, in turn, into three radius-of-curvature groups. Frequency distributions for values of β were then plotted for each subgroup. These had the general appearance of Gaussian curves. In each subgroup all but about five percent of the tracks lay within $\pm 4^\circ$ of the average value for the subgroup. This was considered the acceptable range for pions in the particular subgroup. Mesons outside these ranges were considered to have too great a likelihood of being muons.

About 10 percent of the photographs were judged to have too many tracks to be of use. That is, the tracks were so numerous that they frequently overlapped and were thus difficult, if not impossible, to follow through the aluminum plates. Such pictures were rejected without attempting to discover possible events in order to avoid any bias toward using photographs which appeared to contain events.

A sampling procedure was used to predict the total path in the aluminum. Approximately one-fifth of the 600-odd good photographs were selected at random and used in the sampling. The measurements made on these tracks were also used to determine the energy distribution before the first plate (Fig. 4) and the energy spectrum at the plate centers as a function of number of traversals/Mev (Fig. 7).

It will be noted in Fig. 7 that the meson energies at the plate centers have been divided into three intervals: 25-45 Mev; 45-70 Mev; and 70-100 Mev, with mean energies $[(\sum g/\text{cm}^2 \text{ of aluminum traversed}) \times (\text{energy in Mev})] / (\sum g/\text{cm}^2 \text{ of aluminum traversed})$ of 36, 55, and 82 Mev, respectively. Cross-section determinations were based upon the predicted total g/cm² of aluminum traversed in each of these energy intervals, determined by a direct summation of the sampled path lengths

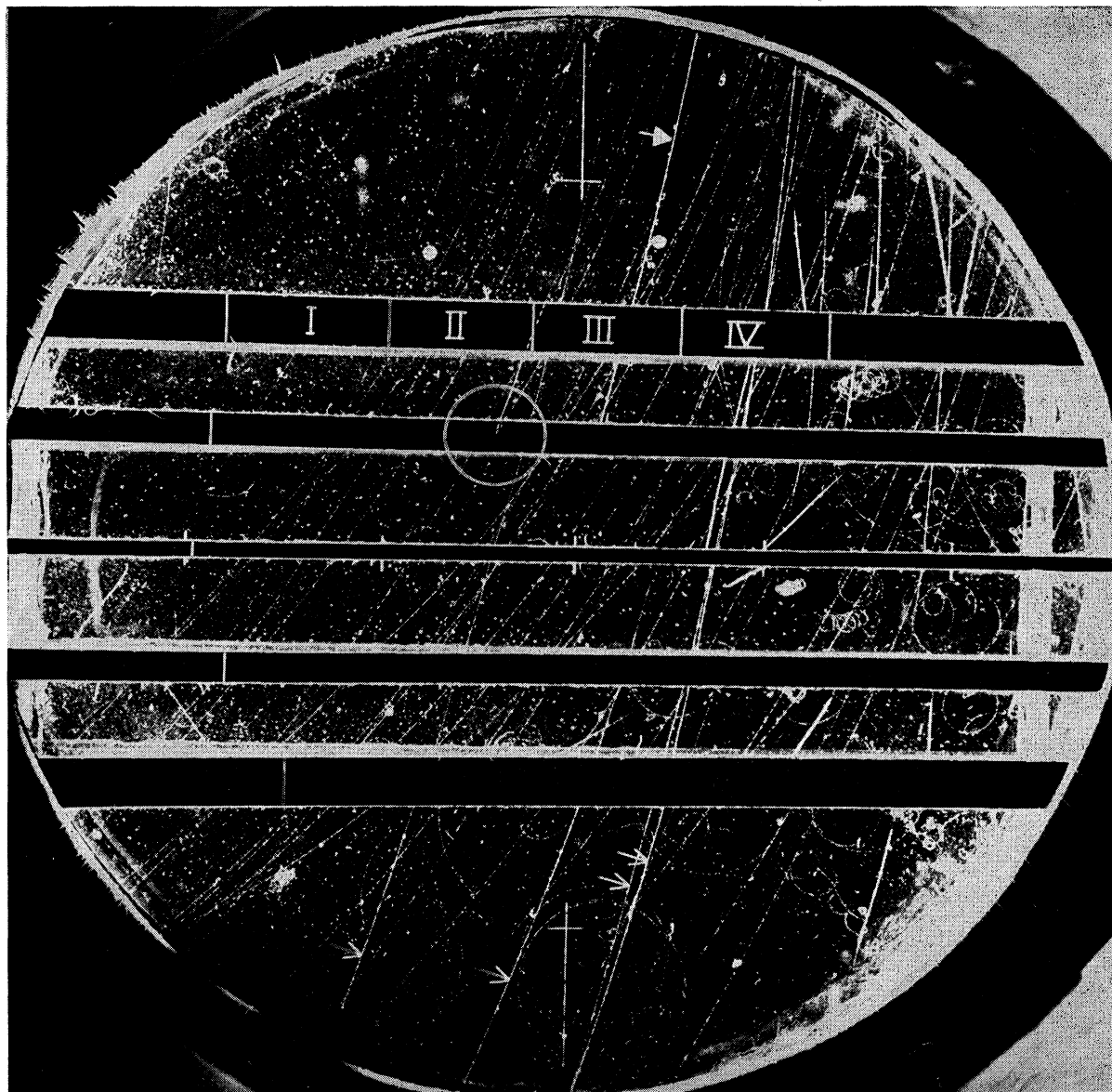


FIG. 6. A representative photograph of chamber. The mesons enter at the bottom in thin, curving, nearly parallel paths. Circled is a 1-prong star; a 42-Mev pion enters the second plate and one disintegration fragment (probably a proton) leaves at an angle of 155° to the direction of the incoming meson. The four open arrows at the bottom indicate energetic protons (>70 Mev) that have traversed all five plates. The single solid arrow at the top points to a slower heavy particle (presumably a proton) that soon stops. The thin, highly curved and spiralled tracks are electrons or (infrequently) positrons. The white bars across the plates have reference to track selection criteria. The crosses at top and bottom center are fiducial marks, spaced twelve inches apart.

within each energy interval and not by integration under the curve of Fig. 7.

The great majority of tracks were enumerated by a "rapid count" procedure; a detailed measurement of each track was not made. It usually was possible by a visual inspection of a stereophotograph to determine whether or not a track met the criteria for acceptance. In doubtful cases—amounting to approximately ten percent of the total number—detailed measurements were made. The rapid count covered all pictures used,

including those gone over in the detailed count under the sampling procedure outlined above. A comparison of the number of tracks enumerated in the detailed count (850) with those in the rapid count (851) covering the same random sample of photographs established the validity of the procedure. 3976 tracks (making 15 359 aluminum plate traversals) were enumerated in the rapid count.

Events (scatters $\geq 10^\circ$, stops, and stars) were looked for by carefully following, in the stereoprojector, each

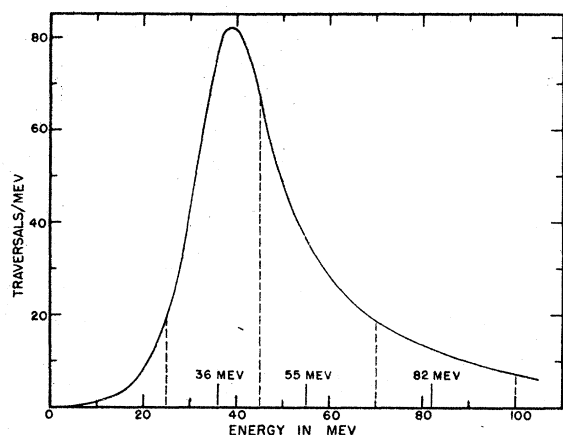


FIG. 7. Spectrum of meson energies at the centers of the aluminum plates as a function of single plate traversals/Mev. These data are based upon a sample of 628 incoming tracks. No correction for muon contamination have been made. The dashed vertical lines indicate the three energy intervals (25-45, 45-70, and 70-100 Mev) into which the data were divided for cross-section determinations. The mean energy for each interval is also indicated.

of the 3976 tracks on its path through the aluminum until it either; (1) successfully traversed the five plates, (2) finally traveled out of the acceptable region, or (3) initiated an event in one of the plates. (Rarely, a pion would decay into a muon between plates. Plate traversals by such muons were not, of course, considered.) Every pion initiating an event (3) was measured in detail. In addition, the position and characteristics of the event itself were determined, especially the angular relationship of the incoming and outgoing tracks. The coincidence of incoming and scattered meson, or incoming meson and outgoing disintegration fragments, within an aluminum plate was carefully verified. This could be done to within ± 0.1 inch vertically and ± 0.05 inch, or better, horizontally. Stops were examined carefully to be certain that no nearby tracks might have originated from the place of disappearance. As a check on the reliability with which tracks and events were counted, five percent of the photographs were examined independently by two different persons. There was essential agreement between the independent counts.

An important point is that, although it was possible to distinguish a scattered meson from a 1-prong disintegration by the difference in ionization, it was not usually possible to establish the scattered meson's or disintegration (star) fragment's energy with precision. This was because of the short path length and the gas turbulence between plates. In a few exceptional cases where the scattered meson or star fragment entered the region before the first plate or after the fifth plate, good curvature measurements could be made. There were not enough of these to be statistically significant. In most cases, order-of-magnitude estimates of energy were possible, particularly in the case of star fragments,

by observing the ionization of the track and/or the change in ionization after passing through an aluminum plate.

MESON BEAM CONTAMINATION

Not all the particles entering the cloud chamber were pi-mesons. It was necessary, of course, either to be able to recognize the contaminating particles or to have information available from which their numbers could be determined in order to evaluate the cross sections correctly. Among the possible ionizing contaminants were protons (and heavier particles), mu-mesons, and positrons. Except for a small background of extraneous tracks produced in the chamber by them, the non-ionizing neutrons and gamma rays presented no difficulty. The few negative particles, presumably electrons, presented no problem either, since they were readily detected by their negative curvatures.

Protons constituted approximately one-fourth of the particles in the beam and were differentiated from mesons by their much higher specific ionization and/or greater radius of curvature. While protons are readily distinguished from pions of the same $B\rho$, muons and positrons are not. For the $B\rho$ range of values of interest in this experiment, pions have a specific ionization not more than 150 percent that of muons of the same radius and not more than two times that for positrons (or electrons) of the same radius. For this reason it was not possible to distinguish the latter two particles from pions. The extent of the muon and positron contamination was determined indirectly.

The muons in the meson beam originated from the decay of pions in flight. In principle it is possible to determine the muons expected to enter the chamber if, among other things, one knows the experimental geometry and the pion beam intensity, energy spectrum, and decay constant. In practice it was necessary to use a number of simplifying mathematical approximations and to make certain assumptions concerning the pion beam intensity and energy spectrum. The mean life of the positive pi-meson was taken to be 2.55×10^{-8} sec.³²⁻³⁸ The "equivalent energy" distribution obtained for the muons contaminating the beam is indicated in Fig. 5. (By "equivalent energy" is meant that energy which a pion would have if it had the same $B\rho$ as that of the muon being considered.) The number of muons was computed to be 13 percent of the total number of pions in the meson beam. Because of large uncertainties that entered into the computations, this figure may be in error by ± 33 percent. The required corrections in the aluminum path lengths are indicated in Table III.

In addition to the indirect calculation of the muon content of the beam, a direct measure of the contamination was attempted in two ways: (1) by ascertaining

³² Chamberlain, Mozley, Steinberger, and Wiegand, Phys. Rev. **79**, 394 (1950).

³³ Jakobson, Schulz, and Steinberger, Phys. Rev. **81**, 894 (1951).

³⁴ C. E. Wiegand, Phys. Rev. **83**, 1085 (1951).

³⁵ W. L. Kraushaar, Phys. Rev. **86**, 513 (1952).

the ratio of muons to pions stopped in nuclear emulsions placed in the beam and (2) by counting the π - μ decays occurring before the first plate in the chamber, inferring from these data the total number of pions which must have entered and comparing the inferred number with the number obtained by actual count. The statistics obtained with these methods were too poor to do more than indicate no lack of agreement with the calculated contamination.

It has been possible to place an upper limit on the positron contamination. This limit was obtained by imagining all the particles in the beam that were accepted as mesons to have been positrons instead, and computing, from data available in Heitler,³⁶ the number of times these positrons would be expected to radiate more than three-fourths of their energy in traversing an aluminum plate. Any positron undergoing such a radiative loss would have emerged from the plate with its radius of curvature reduced in direct proportion to its loss of energy, but with no significant change in its specific ionization; no such events were observed. A pion suffering such a large change in radius would also undergo a large and discernible change in specific ionization.

GEOMETRICAL CORRECTIONS

One observes three types of meson-induced events in the aluminum plates: (1) scatters, (2), disintegrations or "stars," and (3) stops. Type (3) presumably might represent: either (a) a real stop involving charge-exchange scattering and the emission of a neutral pion and no charged particles; (b) a real stop involving meson capture and the subsequent emission of neutrons and slow charged particles of insufficient energy to escape the aluminum; or (c) a "pseudo" stop, corresponding to types 1 or 2 above, in which the outgoing charged particles are hidden by the geometry. It is possible, in principle at least, to take the observed events of types 1 and 2 and calculate from geometrical considerations the most probable additional number of events which would have appeared as pseudo stops. Where one is dealing with pions of positive charge few, if any, real stops corresponding to case (b) are expected. One imagines the incoming positive pion to be absorbed by a neutron within the nucleus and to give rise to at least one fast proton, which evolves into a star of at least one prong. Then the difference between the observed stops (3) and the number of pseudostops (c) predicted by geometrically-based calculations should approximate the number corresponding to case (a), charge-exchange scattering. Even in case (a), of course, a neutron is converted into a proton which, if given sufficient energy, will escape and give rise to a 1-prong star.

By idealizing the geometry somewhat and constructing a simple "analog computer" (Fig. 8), the

³⁶ W. Heitler, *The Quantum Theory of Radiation* (Oxford University Press, London, 1944), second edition.

evaluation of the geometrical corrections was made with a minimum of effort. The procedure used is summarized in Appendix I.

ERRORS

The probable errors in the energy determinations are estimated to have been less than five percent; this is much less than the width of the energy groupings used. Errors in cross-section determinations were in most cases much less than the statistical uncertainties.

The important quantities bearing upon the accuracy of the energy determinations are: mass of the meson, radius of curvature, magnetic field strength, rate of energy loss in aluminum, and path length in aluminum. The present uncertainty in the positive pion mass is about one percent.^{37,38} The true radius of curvature ρ of a track may be obscured by multiple Coulomb scattering in the gas, turbulence in the gas, and errors in fitting template curves to the tracks. The probable error in ρ owing to these causes is estimated to have been about three percent. The maximum uncertainty in the magnetic field intensity B was three percent. The probable error in energy owing to the errors in $B\rho$ is estimated to have been less than five percent.

Measurements were only made on tracks before they entered the first plate. Between plates the separation was too small, and the turbulence too great to permit satisfactory measurements there. In order to fix the energy of a meson beyond the first plate, i.e., at the centers of succeeding plates, it was necessary to calculate the loss of energy by ionization in the aluminum and to subtract this loss from the meson's energy before it entered the first plate. Errors in energy introduced by ionization loss calculations were less than one percent.

The largest uncertainties in the cross sections derive from the statistics and are indicated in Table I. A

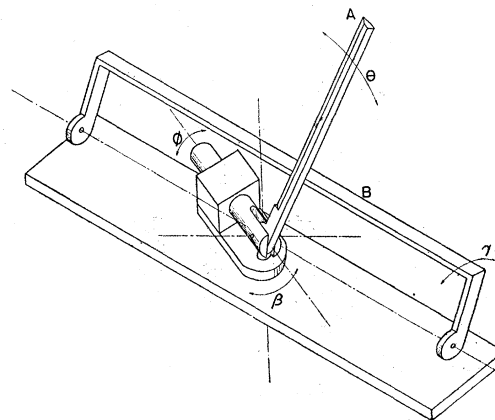


FIG. 8. "Analog computer." This device aided in evaluating the geometrical corrections by determining the weighting factors to be applied to the several kinds of events.

³⁷ W. F. Cartwright, *Phys. Rev.* **82**, 460 (1951).

³⁸ W. H. Barkas, *Am. J. Phys.* **20**, 5 (1952).

$f_{s_0}^{(i)}$ = fraction of time the i th observed scatter is expected to have appeared as an observed pseudostop.

$f_{1_0}^{(i)}$ = fraction of time the i th observed 1-prong star is expected to have appeared as an observed pseudostop.

$f_{2_0}^{(i)}$ = fraction of time the i th observed 2-prong star is expected to have appeared as an observed pseudostop.

$f_{21}^{(i)}$ = fraction of time the i th observed 2-prong star is expected to have appeared as an observed pseudo 1-prong star.

Having defined the above quantities, one may write down the following relations:

$$N_S r_{s_0} = \sum f_{s_0}^{(i)} / (1 - f_{s_0}^{(i)}),$$

$$N_2 r_{2_0} = \sum f_{2_0}^{(i)} / (1 - f_{2_0}^{(i)} - f_{21}^{(i)}),$$

$$N_2 r_{21} = \sum f_{21}^{(i)} / (1 - f_{2_0}^{(i)} - f_{21}^{(i)}),$$

$$(N_1 + N_{2r_{21}}) r_{1_0} = \sum f_{1_0}^{(i)} / (1 - f_{1_0}^{(i)}).$$

(The summations are carried over all the events in the categories for which the particular $f^{(i)}$'s do not vanish.)

It is now possible to calculate the value of the N 's providing one makes the following two assumptions: (1) $N_0 = 0$, i.e., there were no real — as opposed to pseudostops; (2) $r_{1_0} \approx \bar{r}_{1_0}$, where

$$\bar{r}_{1_0} = [f_{1_0}^{(i)} / (1 - f_{1_0}^{(i)})]_{Av}.$$

One may now write

$$N_S = [n_S + N_S r_{s_0}],$$

$$N_0 = 0,$$

$$N_1 = [n_1 + (N_1 + N_{2r_{21}}) r_{1_0}] - N_{2r_{21}} (1 + \bar{r}_{1_0}),$$

$$N_2 = n_2 + N_{2r_{20}} + N_{2r_{21}}.$$

The results of these computations are displayed in Table I. The standard deviations have been determined from the number of events of each kind observed; i.e., $N_S \cdot [1 \pm (1/n_S)^{1/2}]$, $N_1 \cdot [1 \pm (1/n_1)^{1/2}]$, and $N_2 \cdot [1 \pm (1/n_2)^{1/2}]$.

The Mean Life of Negative μ Mesons Stopped in Iron* †

A. H. BENADE ‡

Washington University, St. Louis, Missouri

(Received April 30, 1953)

The mean life of negative cosmic-ray μ mesons stopping in an iron absorber has been found experimentally to be 0.21 ± 0.06 μ sec. The upper limit to the mean number of neutrons produced is very roughly one per meson captured by an iron nucleus.

THE development of hydrogenous scintillating liquids suitable for efficient and fast detection of neutrons in the 1 to 10-Mev range¹ has made it possible to extend measurements of the mean life of stopped negative μ mesons to materials of higher atomic number than could be studied previously with Geiger counters.² The scintillator is used to detect neutrons (or gamma rays) resulting from the interaction of the stopped meson with the nucleus. The time delay is measured between the arrival of the meson in the stopping material and the detection of the nuclear disintegration. An extensive experiment of this sort has recently been reported by the Princeton group.³ The present experiment was completed before publication of the Princeton measurements on iron. Its result is in agreement with their more precise result, constituting an independent confirmation.

Figure 1 shows the geometrical disposition of the counter tubes and the absorber and also the nature of the input circuits. Counter trays A_1 and A_2 each

contain ten brass-walled Geiger counters of 1 inch diameter by 25.4 cm effective length, which are connected to a two-stage pulse amplifier. Between these two trays is an iron filter 15.2 cm thick, and below them is the absorber, a 30.5 cm cube of iron. Through the middle of this cube runs a brass cylinder 2 in. in diameter and 31.6 cm long, containing a scintillating solution of 2 grams/liter of terphenyl in xylene. Two EMI 5311 photomultiplier tubes look into the ends of the column of liquid. The amplified outputs, B_1 and B_2 , of these tubes are connected in coincidence to suppress noise. Underneath the absorber cube is a third tray C similar to the A_1 and A_2 trays, and containing twelve Geiger counters of 1 in. diameter by 50.8 cm effective length. This C tray covers most of the solid angle subtended by the absorber cube at the $A_1 A_2$ telescope.

Pulses from the A_1 and A_2 trays are fed to a coincidence circuit⁴ of 0.22- μ sec resolving time, which produces an output signal that is fixed in time relative to the earlier of the two input pulses. This output signal is used to initiate the timing process of a ten-channel delay discriminator⁵ which measures the time between signals from the A trays and the scintillation counter B . In order to minimize the timing changes caused by variations in pulse height, the amplified $B_1 B_2$ coinci-

* Based on Washington University thesis, June, 1952.

† Assisted by the joint program of the U. S. Office of Naval Research and the U. S. Atomic Energy Commission.

‡ Now at Case Institute of Technology, Cleveland, Ohio.

¹ Jastram, Benade, Cleland, and Hughes, Phys. Rev. **81**, 327 (1951).

² T. Sigurgeirsson and A. Yamakawa, Phys. Rev. **71**, 319 (1947); H. K. Ticho, Phys. Rev. **74**, 1337 (1948); A. H. Benade and R. D. Sard, Phys. Rev. **76**, 488 (1949).

³ Keuffel, Harrison, Godfrey, and Reynolds, Phys. Rev. **87**, 942 (1952).

⁴ Such a circuit was first used by M. L. Sands [Rossi, Sands, and Sard, Phys. Rev. **72**, 120 (1947)].

⁵ The time base of this discriminator is adapted from the Los Alamos Model 300 Sweep.

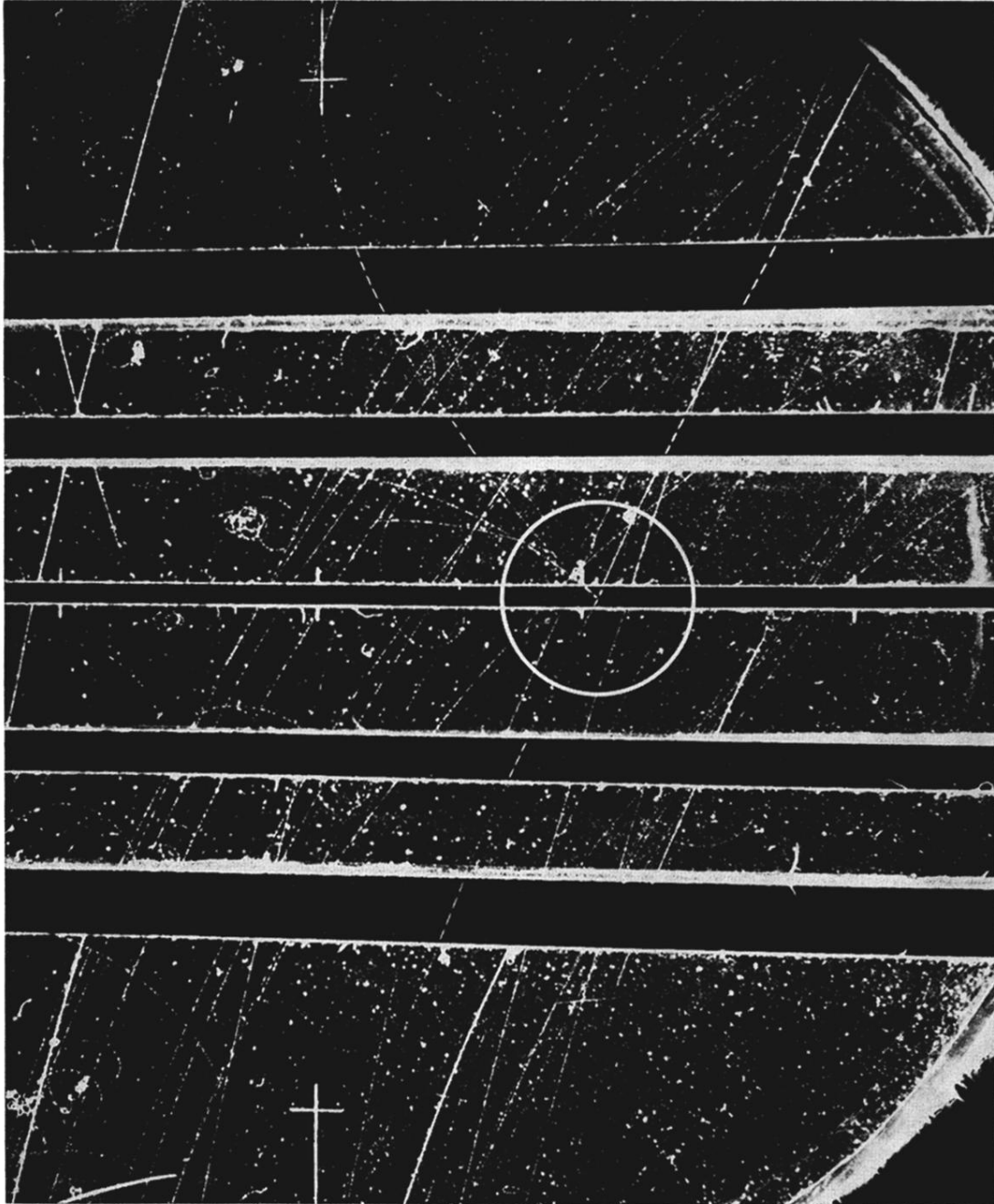


FIG. 3. A charge-exchange scatter. An 88-Mev pion enters the third plate and, presumably, suffers a charge-exchange scatter. A 51-Mev proton is ejected at 6° to the forward direction; the neutral pion decays and causes a 70-Mev electron-positron pair to leave the plate at 75° to the forward direction. (The electron takes 28 Mev and the positron, 42 Mev.)

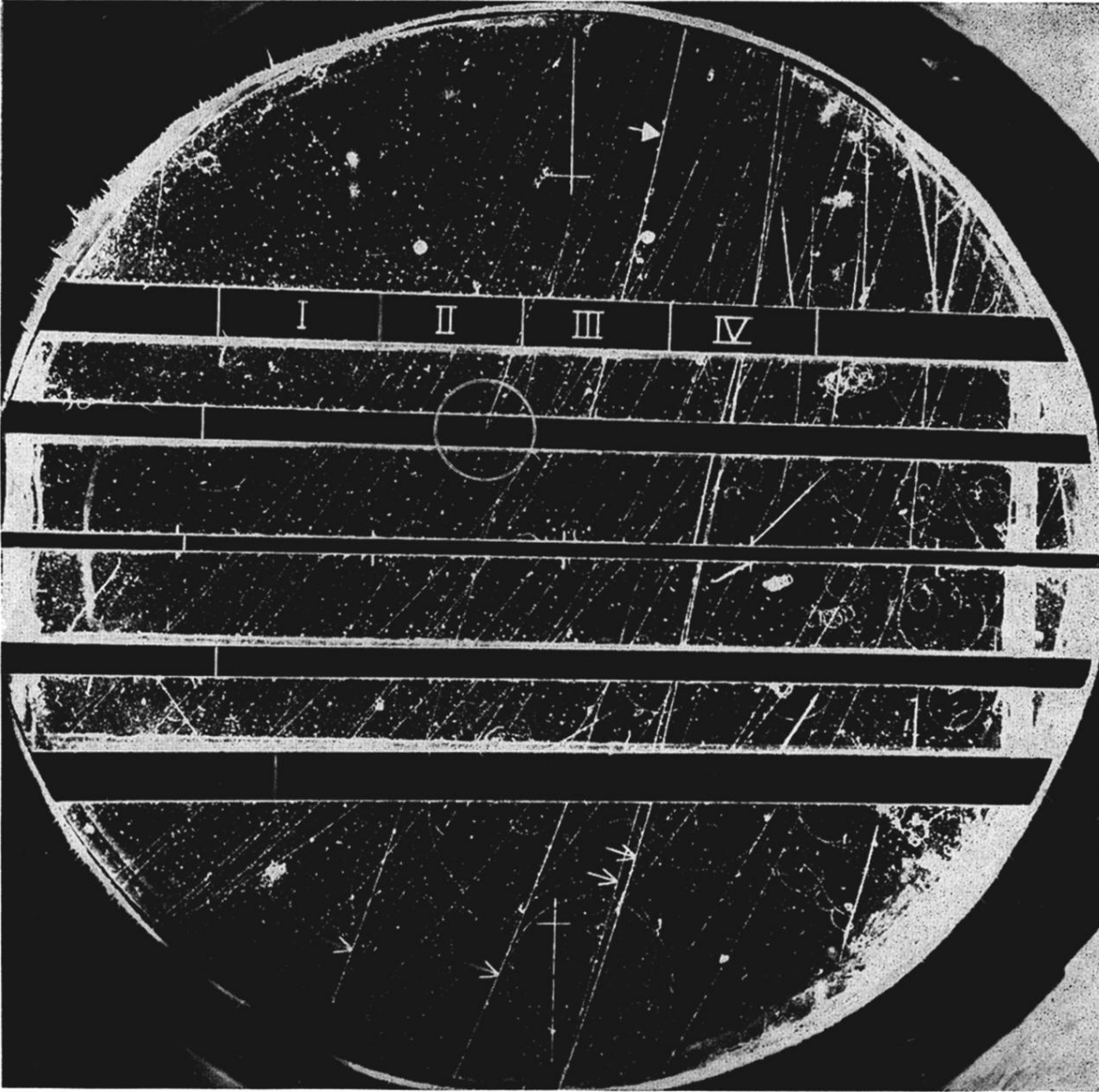


FIG. 6. A representative photograph of chamber. The mesons enter at the bottom in thin, curving, nearly parallel paths. Circled is a 1-prong star; a 42-Mev pion enters the second plate and one disintegration fragment (probably a proton) leaves at an angle of 155° to the direction of the incoming meson. The four open arrows at the bottom indicate energetic protons (>70 Mev) that have traversed all five plates. The single solid arrow at the top points to a slower heavy particle (presumably a proton) that soon stops. The thin, highly curved and spiralled tracks are electrons or (infrequently) positrons. The white bars across the plates have reference to track selection criteria. The crosses at top and bottom center are fiducial marks, spaced twelve inches apart.